Mechanism of Dissolution of Sparingly Soluble Electrolytes

Ruikang Tang,[†] George H. Nancollas,*[,†] and Christine A. Orme[‡]

Department of Chemistry, Natural Sciences Complex, University at Buffalo, The State University of New York, Buffalo, New York 14260, and Department of Chemistry and Materials Sciences, Lawrence Livermore National Laboratory, California 94550

Received January 8, 2001

Abstract: Recent constant composition dissolution studies of sparingly soluble calcium phosphates have revealed an interesting and unusual behavior in that the rates decreased, eventually resulting in effective suppression, even though the solutions remained undersaturated. Contrary to traditional theories of dissolution, these experimental results indicated the importance of not only the particle size on the dissolution rate but also the participation of critical phenomena. In these theories, it is assumed that when the dissolution reactions are initiated, they continue spontaneously until all solid phase has disappeared. In terms of these mechanisms, there are no critical phenomena in the dissolution mechanism. Although the crystal size decreases during dissolution, when the reaction is controlled by polypitting (formation and growth of pits), the edge free energy increases at the very first stage due to the creation of pits and dissolution steps. The constant composition experimental results demonstrate the development of surface roughness as the dissolution steps are formed, implying an increase of the total edge length during the reactions. In an exactly analogous mechanism to crystal growth, the participation of critical conditions involving dissolution steps is a possibility. In contrast to crystal growth, dissolution is a process of size reduction and, when the particle size is sufficiently reduced, critical phenomena become important so that the influence of size must be taken into consideration. This paper proposes such a model for dissolution reactions, and although these unusual phenomena probably apply to all mineral phases, they are more evident for sparingly soluble electrolytes in which the critical conditions are attained much more readily.

Introduction

In terms of well-established theories of crystallization, when critical condition are attained, nucleation and growth processes are initiated and continue spontaneously in supersaturated solutions. $\Delta G(r)$, the change of Gibbs free energy for the formation of a two-dimensional nucleus of radius r, is given by eq 1

$$\Delta G(r) = \frac{\pi r^2}{\Omega}\Delta g + 2\pi r\gamma \qquad (1)$$

in which Δg is the change in Gibbs energy per growth unit (atom/molecule) from liquid to solid, γ *is* the edge-free energy, and Ω is the area occupied by each growth unit. In eq 1, the first term on the right-hand side represents the supersaturation driven decrease of free energy during the phasetransformation (nucleation) while the second term describes the increase of the edge-free energy accompanying the creation of new nuclei. The critical size, r^*, obtained by setting $\partial(\Delta G)/\partial(r) = 0$, is given by eq 2

$$r^* = \frac{\gamma\Omega}{|\Delta g|} \qquad (2)$$

In comparison to the more mature theories of crystal growth, dissolution has received much less attention despite its importance.[1−3] Although recent progress in dissolution studies by in situ atomic force microscopy (AFM)[4,5] and scanning electrochemical microscopy (SECM)[6−8] have revealed the importance of pit formation and development, the second term on the right-hand side of eq 1 is either ignored or assumed to be negative in most dissolution studies.[9−11] This is partly because dissolution results in a reduction of crystal size/interface area and partly because crystal edges are always ready sources of dissolution steps at which dissolution can take place.[12,13]

In most kinetic studies, the dissolution rate has been expressed analogously to crystal growth by eq 3,[11,14,15]

$$R(J) = w\beta(c_e - c) \qquad (3)$$

where w is the slope of vicinal hillocks, β is the face kinetic

[†] University at Buffalo, The State University of New York.
[‡] Lawrence Livermore National Laboratory.

(1) Stumm, W. *Chemistry of the Solid-Water Interface*; Wiley: New York, 1992.
(2) Lowenstam, H. A.; Weiner, S. *On Biomineralization*; Oxford University Press: Oxford, 1989.
(3) Nancollas, G. H. *Biological Mineralization and Demineralization*; Springer: Berlin, Heidelberg, 1982.
(4) Malkin, A. J.; Kuznetsov, Yu. G.; Glantz, W.; Mcpherson, A. *J. Phys. Chem.* **1996**, *100*, 11736.
(5) Jones, C. E.; Macpherson, J. V.; Unwin, P. R. *J. Phys. Chem. B* **2000**, *104*, 2351.
(6) Macpherson, J. V.; Unwin, P. R. *J. Phys. Chem.* **1994**, *98*, 11764.
(7) Macherson, J. V.; Unwin, P. R.; Hillier A. C.; Bard, A. J. *J. Am. Chem. Soc.* **1996**, *118*, 6445.
(8) Macherson, J. V.; Umwin, P. R. *Chem. Soc. Rev.* **1995**, *24*, 109.
(9) Hartman, P. *Crystal Growth: An introductin*; North-Holland: Amsterdam-London-New York-Tokyo, 1975.
(10) Hurle, D. T. J. *Handbook of Crystal Growth*; North-Holland: Amsterdam-London-New York-Tokyo, 1993.
(11) Chernov, A. A. *Prog. Cryst. Growth Charact. Mater.* **1993**, *26*, 121.
(12) Hirth, J. P.; Pound, G. M. *J. Chem. Phys.* **1957**, *26*, 1216.
(13) Surek, T. *J. Cryst. Growth* **1972**, *13/14*, 19.
(14) Chernov, A. A. *Modern Crystallography III*, *Springer Series Solid State*, Vol. 36; Springer: Heidelberg, 1984.

10.1021/ja010064p CCC: $20.00
Published on Web 05/18/2001

coefficient (a constant for each crystallite face), and c and c_e are the concentrations at time t and at equilibrium, respectively. Equation 3 implies that the dissolution rate should be constant when the undersaturation is maintained. Recently, however, it has been shown that this simple representation of dissolution is unsatisfactory as exemplified by the different mechanisms that have been proposed for the same reaction;[16−19] clearly dissolution cannot be considered simply by analogy to crystal growth.[20,21] Constant composition studies of the dissolution of the calcium phosphates have shown that the rates decrease markedly with time despite a sustained undersaturation.[20−25] In the present work, the rates approach zero even though crystals remain in the undersaturated solutions, an analogous phenomenon to that observed in crystallization in which nucleation/growth may not occur below the critical condition requirements. Our studies have also shown that dissolution of crystals that have undergone suppressed dissolution can resume when the degree of undersaturation is changed to either higher or lower values.[21] Clearly, these results cannot be interpreted in term of current dissolution models and it is suggested that the second term of eq 1 may assume positive values under certain conditions requiring the introduction of a critical condition for dissolution.

In the present work, a number of calcium phosphates, namely, dicalcium phosphate dihydrate ($CaHPO_4 \cdot 2H_2O$, DCPD), β-tricalcium phosphate ($Ca_3(PO_4)_2$, TCP), octacalcium phosphate ($Ca_8H_2(PO_4)_6 \cdot 5H_2O$, OCP), and hydroxyapatite ($Ca_{10}(PO_4)_6(OH)_2$, HAP), have been investigated to test this dissolution model. These phases were selected for study because of their importance in biomineralization.[2,3,26−28]

Experiment and Methods

In the constant composition (CC) method, multiple titrant solutions were added simultaneously to the reaction solutions to compensate for the changes of lattice ion concentrations during the reactions.[29,30] Titrants having stoichiometries matching those of the dissolving phases while taking into account dilution effects were prepared. The dissolution experiments, initiated by the introduction of known amounts of crystal seeds, were conducted in magnetically stirred (450 rpm) double-walled Pyrex vessels thermostated at 37.0 ± 0.1 °C. Undersaturated solutions were prepared by slowly mixing calcium chloride and potassium dihydrogen phosphate with sodium chloride to maintain the ionic strength, I, at 0.15 mol L^{-1}. The pH was adjusted to the desired value between 4.00 and 6.80 using potassium hydroxide or hydrochloric acid. Titrant addition was trigged by a potentiometer (Orion 720A, U.K.) incorporating a glass (Orion No. 91-01, U.K.) and reference (Orion 900100, U.K.) electrode. During the dissolution, the potential of the potentiometer was constantly compared with a preset value and the difference, or error signal, activated motor-driven titrant burets. Thus, a constant thermodynamic driving force for the dissolution was maintained. During the reactions, slurry samples were periodically withdrawn and filtered (0.22 μm Millipore filter) and the solutions were analyzed for total calcium (atomic absorption) and phosphate (spectrophotometrically as the vanadomolybdate complex); during the experiments concentrations remained constant to within 1%.

The overall crystal dissolution flux rate, J (expressed as moles of dissolved crystals per min per m^2 of total seeds), was calculated from the recorded time/titrant volume curves using eq 4.

$$J = \frac{T_{Ca}{}^{w}}{N_{Ca} A_T} \frac{dV}{dt} \tag{4}$$

In eq 4, the rate was normalized with respect to the seed surface area, A_T. $T_{Ca}{}^{w}$ is the total molar calcium concentration in the undersaturated solution, dV/dt is the gradient of the titrant curves, and N_{Ca} is the number of calcium ions in the formula unit of the dissolving phase. The initial value of A_T was calculated from the specific surface area of the seeds, and the subsequent values during dissolution were estimated from the dissolution model described previously.[21,31] To test model theories, the linear rate of dissolution, R, was calculated from the flux rate as described previously.[21,31]

The relative undersaturation, σ, is given by eq 5

$$\sigma = 1 - S = 1 - \left[\frac{IP}{K_{sp}}\right]^{1/\nu} \tag{5}$$

where S is the undersaturation ratio, ν is the number of ions in a formula unit of the dissolving phase, and IP and K_{sp} are the ionic activity and solubility products, respectively. Solution speciation calculations were made using the extended Debye−Hückel equation proposed by Davies [32,33] from mass balance expressions for total calcium and total phosphate with appropriate equilibrium constants by successive approximation for the ionic strength. Values adopted for the dissociation constants of phosphoric acid were $K_1 = 6.22 \times 10^{-3}$,[22] $K_2 = 6.59 \times 10^{-8}$,[35] and $K_3 = 6.6 \times 10^{-13}$ mol L^{-1},[36] and the water ionic product was 2.40×10^{-14} mol^2 L^{-2}.[37] The formation constants for the ion pairs $CaH_2PO_4^+$, $CaHPO_4$, $CaPO_4^-$, and $CaOH^+$ were taken as 28.1,[20] 589, 1.40×10^6, and 25 L mol^{-1},[38] respectively. The solubility activity products, K_{sp}, of DCPD, TCP, OCP, and HAP were 2.32×10^{-7} mol^2 L^{-2}, 2.83×10^{-30} mol^5 L^{-5}, 2.51×10^{-99} mol^{16} L^{-16}, and 5.52×10^{-118} mol^{18} L^{-18}, respectively.[39,40]

DCPD, OCP, and HAP seed crystals were prepared as described elsewhere,[18,41,42] and TCP was obtained from Clarkson (South Williamsport, PA). All samples were characterized by chemical analysis,[43] infrared, and X-ray diffraction, and specific surface areas were

(15) Sunagawa, I. *Morphology of Crystals*; Terra Sci. Pub. Col.: Tokyo, 1987.
(16) Patel, M. V.; Fox, J. L.; Higuchi, W. I. *J. Dent. Res.* **1987**, *66*, 1425.
(17) Voegel, J. C.; Gumpper, M.; Gramain, Ph. *J. Colloid Interface Sci.* **1989**, *132*, 403.
(18) Christoffersen, J.; Christoffersen, M. *J. Cryst. Growth* **1992**, *121*, 608.
(19) Melikhov, L. V.; Dorozhkin, S. V.; Nikolaev, A. L.; Kozlovskaya, E. D.; Rudin, V. N. *Russ. J. Phys. Chem.* **1990**, *64*, 1746.
(20) Zhang, J.; Nancollas, G. H. *J. Cryst. Growth* **1992**, *123*, 59.
(21) Tang, R.; Nancollas, G. H. *J. Cryst. Growth* **2000**, *212*, 261.
(22) Tang, R.; Wu, W.; Haas, M.; Nancollas, G. H. *Langmuir*, in press.
(23) Budz, J. A.; Nancollas, G. H. *J. Cryst. Growth* **1988**, *91*, 490.
(24) Zhang, J.; Nancollas, G. H. *J. Cryst. Growth* **1992**, *125*, 251.
(25) Zhang, J.; Nancollas, G. H. *J. Phys. Chem.* **1992**, *96*, 5478.
(26) Driessens, F. C. M.; Verbeeck, R. M. H. *Biominerals*; CRC Press: Boca Raton, FL, 1990.
(27) Elliot, J. C. *Structure and Chemistry of the Apatites and Other Calcium Orthophosphates*; Springer-Verlag: Amsterdam-London-New York-Tokyo, 1994.
(28) LeGeros, R. Z. *Calcium Phosphates in Oral Biology and Medicine*; S. Karger: Basel, 1991.
(29) Tomson, M. B.; Nancollas, G. H. *Science* **1978**, *200*, 1059.
(30) Koutsoukos, P.; Amjad, Z.; Tomson, M. B.; Nancollas, G. H. *J. Am. Chem. Soc.* **1980**, *102*, 1553.
(31) Liu, Y. Ph.D. Dissertation, State University of New York at Buffalo, 1996.
(32) Davies, C. W. *Ion Association*; Butterworth: London, 1962.
(33) Robinson, P. A.; Stokes, R. H. *Electrolyte Solutions*, 2nd ed.; Butterworth: London, 1959.
(34) Bates, R. G. *J. Res. Natl. Bur. Stand.* **1951**, *47*, 2236.
(35) Bates, R. G.; Acree, S. F. *J. Res. Natl. Bur. Stand.* **1945**, *34*, 396.
(36) Bjerrum, N.; Unmack, A. K. *Dans. Vidensk. Selsk. Mater.-Fys. Medd.* **1929**, *9*, 1.
(37) Harned, H. S.; Owen, B. B. *The Physical Chemsitry of Electrolytic Solutions*, 3rd ed.; Reinbold: New York, 1958.
(38) Zhang, J.; Ebrahimpour, A.; Nancollas, G. H. *J. Solution Chem.* **1991**, *21*, 455.
(39) Shyu, L. J.; Perez, L.; Zawachi, S. J.; Heughebaert, J. C.; Nancollas, G. H. *J. Dent. Res.* **1982**, *62*, 398.
(40) Tung, M. S.; Eidelman, N.; Sieck, B.; Brown, W. E. *J. Res. Natl. Bur. Stand.* **1988**, *93*, 613.
(41) Brown, W. E.; Lehr, J. R.; Smith, J. P.; Frazier, A. W. *J. Am. Chem. Soc.* **1957**, *79*, 5318.
(42) Marshall, R. W.; Nancollas, G. H. *J. Phys. Chem.* **1969**, *73*, 3838.
(43) Tomson, B. M.; Barone, J. B.; Nancollas, G. H. *At. Absorpt. Newsl.* **1977**, *16*, 117.

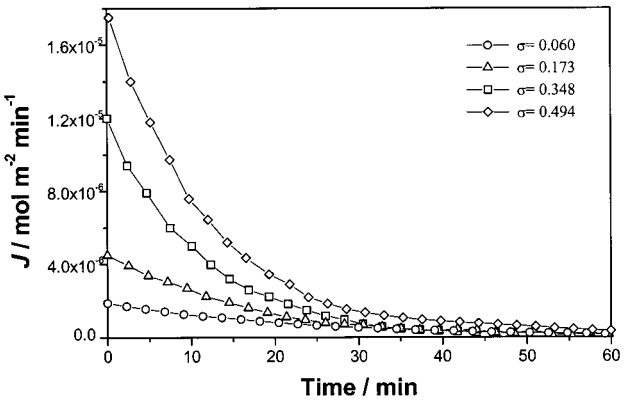

Figure 1. Plots of flux rate (J) against time for DCPD dissolution at different undersaturations.

determined by BET nitrogen adsorption (30:70 N_2/He, Quantasorb II, Quantachrome). [44]

Results and Discussions

Under CC experimental conditions, the term $(c_e - c)$ in eq 3 is maintained constant, and accordingly, the dissolution rate should be constant. However, as shown in Figure 1 the experimental dissolution rates decreased markedly with time, eventually tending to zero. It should be noted that for DCPD dissolution the CC method was capable of quantifying flux rates as low as $10^{-9}-10^{-8}$ mol m^{-2} min^{-1} (the estimated m and β values were approximately 1×10^{-3} and 0.01 cm/s, respectively[11]). When the rates decreased below this limit, the process was regarded as being essentially suppressed. Typically, the dissolution rates of DCPD were reduced to effective suppression in only 2−5 h. At that time, crystallites remained in the undersaturated solutions and the percentage of the dissolved crystals before reaching that stage increased with increasing undersaturation, the values being about 64%, 68%, 73%, and 79% at σ values of 0.060, 0.173, 0.348, and 0.494, respectively. This unexpected dissolution suppression was also observed with the other sparingly soluble calcium phosphates. The effect is expressed more clearly in Figure 2 as a plot of titrant volume as a function of time for OCP dissolution. This figure shows (in dotted lines) the expected titrant volumes that would be obtained if the solid phases completely dissolved. However, only 30%, 45%, and 55% of added OCP seeds underwent dissolution at relative undersaturations of 0.171, 0.352, and 0.525, respectively. The dissolution of TCP behaved similarly. However, if fresh seed crystals were introduced into a suspension in which the reaction had already been suppressed, dissolution of the new crystallites resumed immediately but only to exactly the same extent as for the first part of the experiments.[21] The same phenomenon was observed in repeated dissolution experiments, using ultrapure chemicals (calcium chloride, 99.999%, potassium dihydrogen phosphate, 99.99%, Aldrich Chemical Co., MO, and sodium chloride, 99.999%, Fisher Scientific, NJ).[20,21,45]

Another explanatory factor that must be taken into account is the possibility of hydrolysis leading to calcium phosphate phase transformation under certain conditions.[26−28] In this case, the formation of less soluble surface phases could be interpreted as dissolution inhibition. However, this possibility was ruled out in previous studies on OCP dissolution.[21,46] Here, even stronger experimental proof that dissolution suppression was not due to phase hydrolysis is provided by results for HAP dissolution. If hydrolysis was the reason for dissolution suppression, it should not have been observed for HAP in contrast to the data shown in Figure 3.

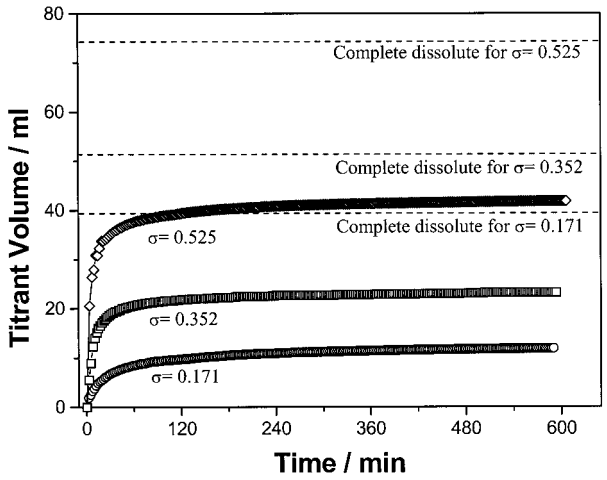

Figure 2. Plots of titrant volume against time for OCP dissolution at different undersatsaturations (pH = 6.00, I = 0.15 mol L^{-1}, 37 °C). The rates decrease virtually to zero; dashed lines show the calculated titrant volume for complete crystal dissolution. The percentages of dissolved crystals increased from 30% at σ = 0.171 to 55% at σ = 0.525.

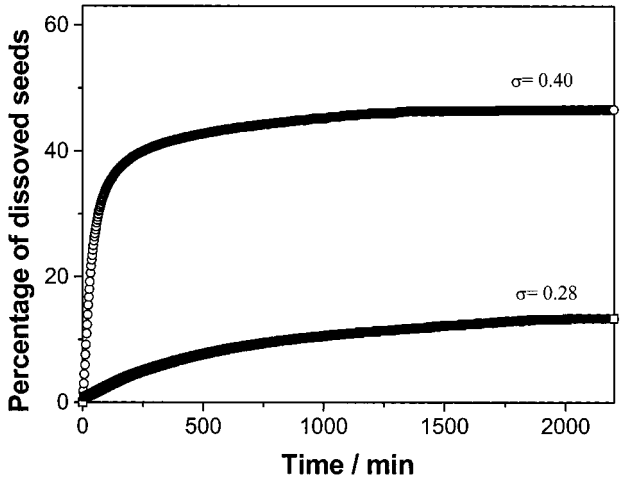

Figure 3. CC curves for HAP, showing incomplete dissolution at constant undersaturation (pH = 4.50, I = 0.15 mol L^{-1}, 37 °C).

Dissolution rate reduction was previously attributed to changes in the number of active dislocations on the crystal surfaces, ρ.[21,47,48] The rate, assumed to be proportional to ρ, would therefore be dependent on the decreasing crystal mass, m. To test this explanation, two OCP crystal seed preparations of different sizes were examined, the larger with a specific surface area of 14.8 m^2 g^{-1} and the smaller at 32.8 m^2 g^{-1}. Plots of the resultant J/J_{int} against $\Delta m/m_{int}$ with $\sigma = 0.171$ are shown in Figure 4 in which, J_{int} and m_{int} are the flux rate and seed mass at zero time, respectively, and Δm represents the dissolved mass. At $\Delta m/m_{int} \leq 0.2$, the plots show a more rapid rate deceleration (J/J_{int}) at the commencement of the small seed

(44) Brunauer, S.; Emmett, P. H.; Teller, E. *J. Am. Chem. Soc.* **1938**, *60*, 309.

(45) Chernov, A. A.; Parvov, V. F.; Kliya, M. O.; Kostomarov, D. V.; Kuzentsov, Yu. G. *Soviet Phys.-Cryst.* **1981**, *26*, 640.

(46) Verbeeck, R. M. H.; Devenyns, J. A. H. *J. Cryst. Growth* **1990**, *102*, 646.

(47) Kirtisinghe, D.; Morris, P. J.; Strickland-Constable, R. F. *J. Cryst. Growth* **1968**, *3/4*, 771.

(48) Treivus, E. B.; Punin, Yu. O.; Ushakovskaya, T. V.; Artamonova, O. I. *Soviet Phys.-Cryst.* **1975**, *20*, 121.

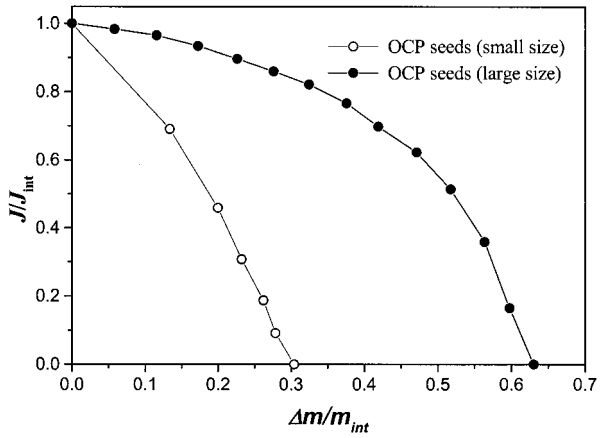

Figure 4. Plots of J/J_{int} against $\Delta m/m_{int}$ for the dissolution of OCP crystals of different sizes at $\sigma = 0.173$.

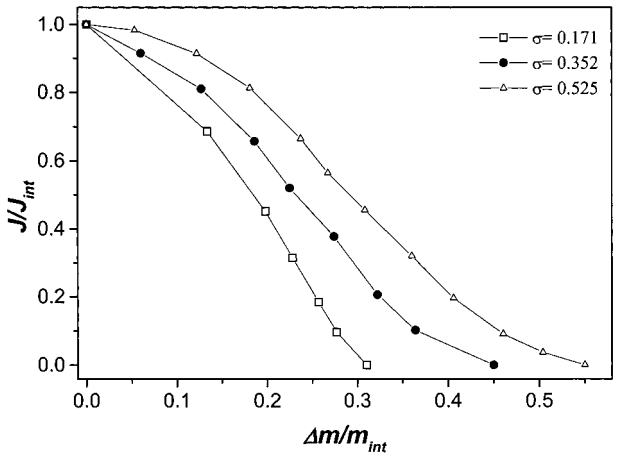

Figure 5. Plots of J/J_{int} against $\Delta m/m_{int}$ for the dissolution of OCP crystals at different undersaturations. The decrease of J/J_{int} at low undersaturation is greater than that at high undersaturation for the same extent of dissolved mass.

dissolution as compared with the larger crystallites. Only when the value of $\Delta m/m_{int}$ increased above 0.3 did J decrease rapidly with loss of mass. Figure 4 shows that although J decreases with Δm, the direct proportionality to be expected from the previously proposed model is absent.[24,25,47−51] In addition, this model cannot be reconciled with the observed decrease in dissolution rate at lower undersaturation that is larger than that at higher driving force for the same mass reduction (Figure 5).

Another important observation was that, if the calcium phosphate crystallites that had undergone the suppressed dissolution were removed by filtration and re-immersed in solutions of the same undersaturations, dissolution did not take place. However, if the undersaturation of the solution was changed to either higher or lower values, dissolution of the remaining crystallites resumed to new well-defined limited extents.[21]

Critical Condition Concepts. Dislocations play an important role in crystal growth in which the first step is the formation of a two-dimensional hillock as a surface nucleus as shown in Figure 6a with an increase of edge energy of $(2\pi r\gamma)$. Previous studies of the calcium phosphates have suggested that dissolution is initiated by surface polynucleation. For an analogous dissolution model, the first step will be the formation of a pit. Thus,

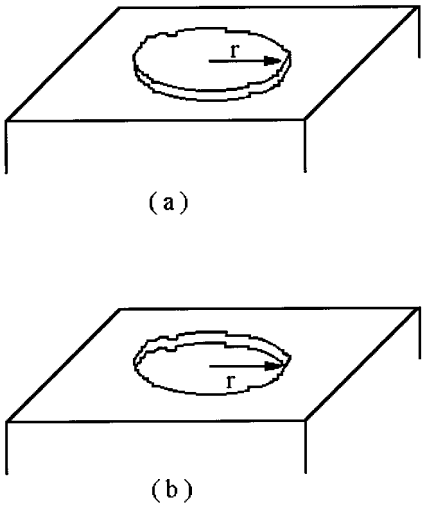

Figure 6. Formation of a hillock (a) and pit (b) during two-dimensional nucleation for growth and dissolution, respectively. Only when the nuclei size, r, reaches the critical value, r^*, does the growth/dissolution proceed spontaneously.

the surface becomes rough and the total edge length and edge-free energy increases with a positive contribution to the second term of eq 1, while the first term remains negative in an undersaturated solution. It is only when a pit of critical size is reached that dissolution becomes spontaneous. Moreover, it can be seen in Table 1 that the second term of eq 1 may not be negative for all possible dissolution cases.

Recent in situ AFM and SECM[6−8] crystal growth and dissolution studies of another biomineral, calcite,[52] and some soluble salts[4,5] confirm a dependence of the growth/dissolution speed (monitored by the movement of growth steps) on step length, l, and its critical value, l_c. These are related by eq 6,[9,10]

$$R(l) = R_\infty\left(1 - \frac{e^{\sigma l_c/l} - 1}{e^{\sigma} - 1}\right) \tag{6}$$

in which R_∞ is the rate when l is infinitely large and the role of l_c is similar to that of r^* for crystal nucleation. Frequently, the dissolution step movement rate can be treated as a reference for the experimental linear/flux dissolution rates.

It is of interest to apply this model to the present situation where, as a result of limitations in current technology, the reaction cannot be followed at a molecular level nor can l_c be measured directly. For dissolution, the maximum length l is limited by the size of the crystals as the dissolution lines must be contained within crystal surfaces, suggesting that crystal size will be a decisive factor. We assume, at constant solution species concentrations, that when the crystal sizes are sufficiently small, the average dissolution step length, l, will be related to the average crystal size, L, i.e., $l \propto L$. Discussion of the dissolution mechanism is thereby facilitated since l_c and L_c may be taken as the average critical step length and crystal size, respectively. Thus, the relationship between the average dissolution rate and the average crystal size can be expressed by eq 7:

$$R = R_\infty\left(1 - \frac{e^{\sigma L_c/L} - 1}{e^{\sigma} - 1}\right) \tag{7}$$

Since the values of R_∞ are unknown in our experiments, they

(49) Eshelby, J. D. *J. Appl. Phys.* **1953**, *24*, 176.
(50) Hirth, J. P.; Frank, F. C. *Philos. Mag.* **1958**, *3*, 1110.
(51) Hirth, J. P.; Lothe, J. *Theroy of Dislocations*; Wiley: New York, 1982.
(52) Teng, H. H.; Dove, P. M.; Orme, C.; Yoreo, J. J. De. *Science* **1998**, *282*, 724.

Table 1. Values of the First and Second Terms of Equation 1 at Different Dissolution Cases

cases		$\Delta g\pi r^2/\Omega$ (first term)	$2\pi r\gamma$ (second term)
dissolution form hillock	away from source	<0	<0
	step containing source	<0	= 0 (edge length is constant) >0 (edge length increases)
pit creation from flat surface		<0	>0
dissolution from dislocation sources with Burger's vectors perpendicular to surface		<0	>0

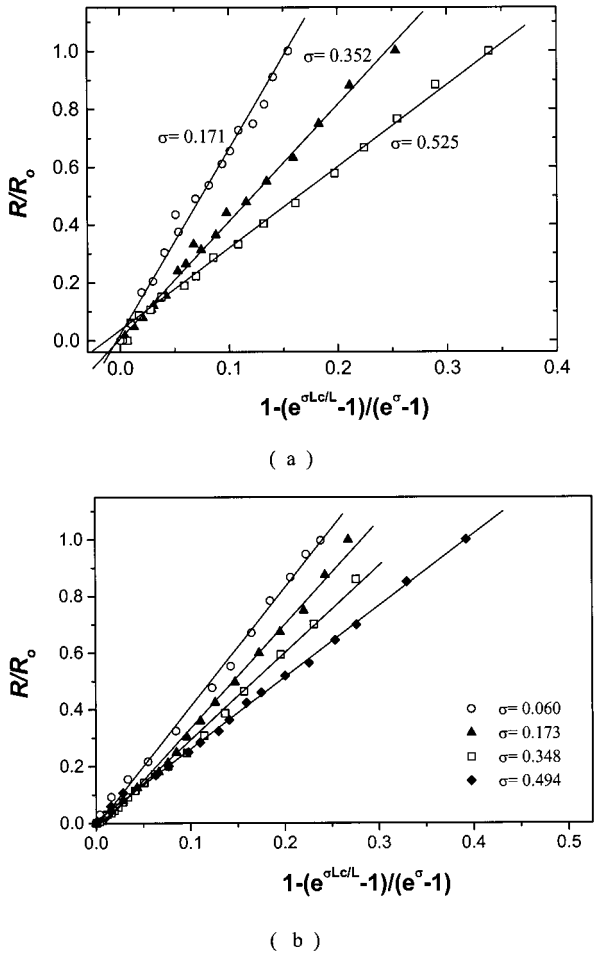

Figure 7. Plots of R/R_0 as a function of $[1 - (e^{\sigma l_c/L} - 1)/(e^{\sigma} - 1)]$ for OCP (a) and DCPD (b). The linearity is in agreement with the proposed model.

are replaced by the initial dissolution rates, R_o. Assuming that $L \approx L^*$ when the dissolution is suppressed, the resulting plots of R/R_o against $[1 - (e^{\sigma L_c/L} - 1)/(e^{\sigma} - 1)]$ for OCP and DCPD at different undersaturations (Figures 7a and 7b, respectively) are seen to be linear, in agreement with this model. During dissolution, the crystallites become smaller and the average lengths of the dissolution steps, l, decrease and approach the critical value, l_c. The resulting decrease in $[1 - (e^{\sigma l_c/l} - 1)/(e^{\sigma} - 1)]$ leads to a decrease in the dissolution rate, R. When the crystal is sufficiently small, the surface geometry of the dissolving crystal does not favor the nucleation of new pits and the limiting dissolution step size is near this critical condition with $[1 - (e^{\sigma l_c/l} - 1)/(e^{\sigma} - 1)] \sim 0$.

For dissolution, Δg is given by eq 8,

$$\Delta g = -kT|\ln S| = -kT|\ln(1 - \sigma)| \qquad (8)$$

where k is Boltzmann's constant and T is the absolute temperature. Combing eqs 2 and 8 shows that r^* and l_c are related to the undersaturation, becoming smaller as the latter increases. Thus, although the values of l may reach their critical limits in solutions of lower undersaturation, causing the reaction to be effectively arrested, they are still greater than the critical value under conditions of higher undersaturation so that the remaining crystallites can continue to dissolve when exposed to such solutions.

SEM crystal growth studies have shown that the critical radius determines the spacing between the dislocation steps, y_o,[9,10,56] and

$$y_o \propto l_c \qquad (9)$$

It can be seen that DCPD crystals that have undergone suppressed dissolution (Figures 8b and 8c) have numerous steps and pits as compared with those prior to dissolution (Figure 8a). These steps and pits have approached their critical limits so that their movement is essentially suppressed. New pits/steps are required for reaction resumption, but their sizes will be limited by that of the equilibrated rough dissolved crystal face, making it difficult to meet the critical requirements. Furthermore, in agreement with the proposed model, the dissolution-suppressed DCPD crystals from solutions of higher undersaturation have much shorter step spacing (Figure 8c) than those at lower undersaturation (Figure 8b). The estimated y_o values are 0.5 and 0.15 μm at σ values of 0.06 and 0.173, respectively; the ratio being 3.3. Combining eqs 2, 8, and 9, the values of y_o, proportional to the term $(1/|\ln(1 - \sigma)|)$, are approximately 16.2 and 5.3 at these two undersaturations; the ratio, 3.1, is close to that estimated from the step spacing. Similar results were obtained for TCP[22] for which SEM revealed the detailed surface condition at dissolution suppression and suggested the relationship between the spacing of the dissolution steps and the critical radius. The good agreement with the proposed model provides added support for the dissolution model presented in this paper.

The present AFM studies of DCPD dissolution in continuously flowing undersaturated solution revealed step movement on the crystal surfaces and the development of pits. Dissolution is initiated and controlled by the formation and subsequent growth of pits, which become larger and deeper during the reaction until they intersect. New smaller pits are then nucleated on the flat terraces, but not all the pits contribute to the dissolution process. Figures 9a and 9b show that in the dissolution of DCPD at $\sigma = 0.060$ only the relatively large pits/steps (G) contribute to dissolution, whereas although the smaller ones (S) exist on the surface, they are stationary and do not appear to contribute to the reaction. These inert pits/steps remain on the surface until replaced by other, "active", dissolution steps. When these small pits dominate the crystal surface, the

(53) Land, T. A.; Yoreo, J. J. De. *J. Cryst. Growth* **2000**, *208*, 623.
(54) Yoreo, J. J. De.; Land, T. A.; Lee, J. D. *Phys. Rev. Lett.* **1997**, *78*, 4462.
(55) Land, T. A.; Martin, T. L.; Potapenko, S.; Palmore, G. T.; Yoreo, J. J. De. *Nature* **1999**, *399*, 442.
(56) Chernov. A. A. *Sov. Phys.* **1961**, *4*, 116.

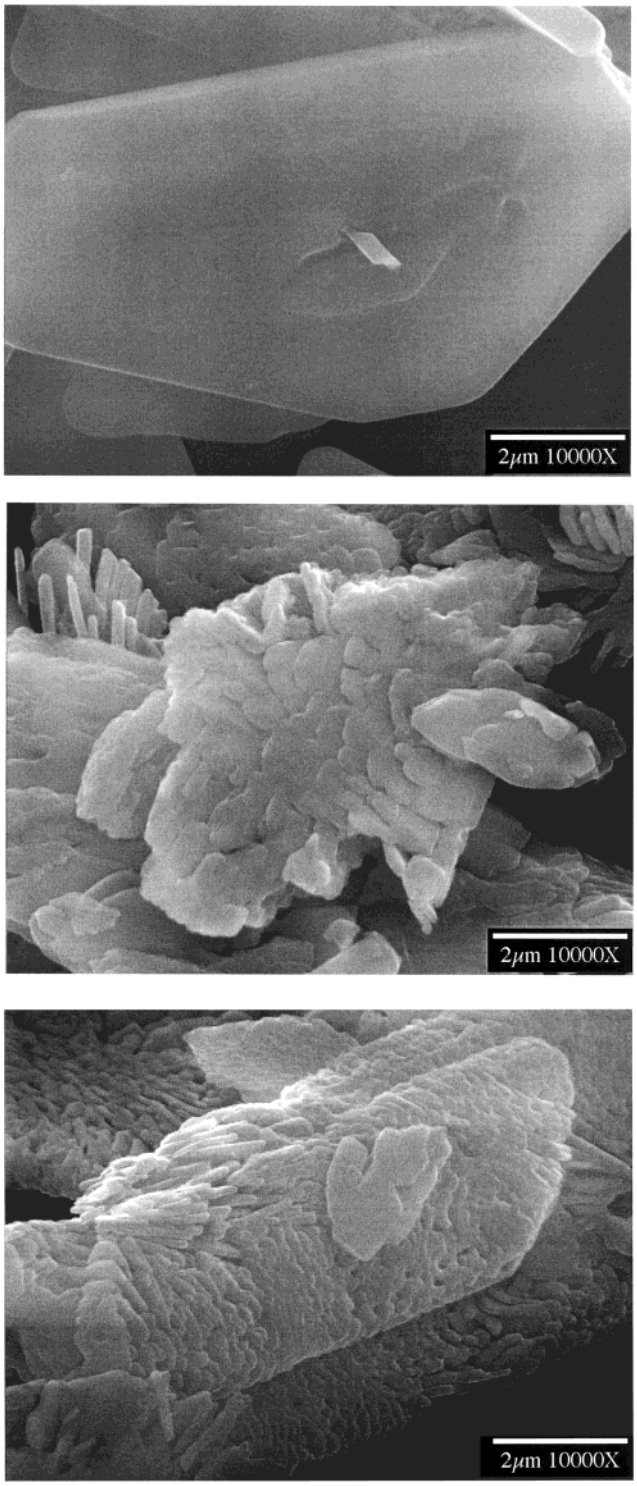

Figure 8. SEM of DCPD crystal seeds (a) and those remaining after dissolution termination (b) at $\sigma = 0.060$ and (c) 0.173.

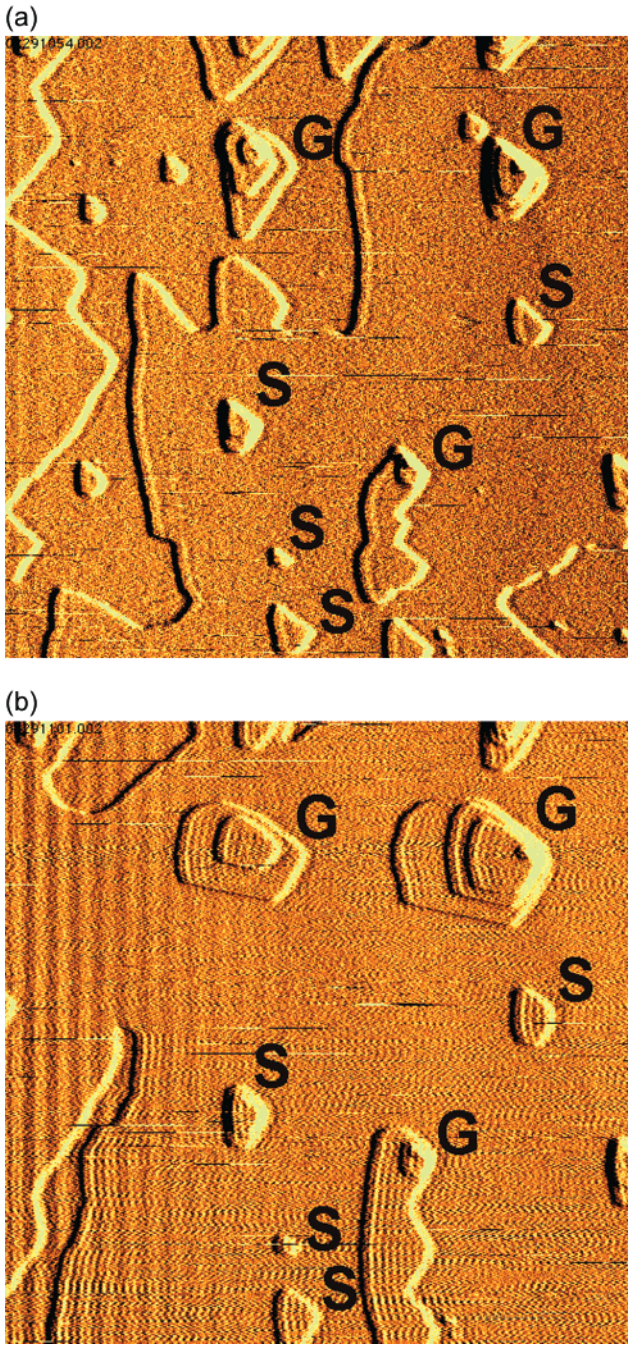

Figure 9. DCPD dissolution at $\sigma = 0.060$ initiated by the formation and growth of pits. The large pits (G) develop during the experiment while the small pits (S) are at a standstill, indicating a relationship between pit growth and critical size. The interval between a and b is 7 min and the image scales are 5×5 μm.

dissolution rate is reduced to near zero as in the CC kinetic experiments. At $\sigma = 0.060$, the sizes of these small pits are about 0.3−0.5 μm, in agreement with the SEM observation, suggesting that no "active" pits form on the dissolution-suppressed surfaces with $y_o \sim 0.45$ μm. This result further supports the relationship between the dissolution rate and pit/step size, and it is also interesting to note that, for the same change in L (or crystal mass, m), l_c at low undersaturation is greater than that at higher σ values. The change in the term $[1 - (e^{\sigma L_c/L} - 1)/(e^{\sigma} - 1)]$ is greater and the decrease in dissolution rate is therefore more noticeable, in agreement with the present results and those reported previously.[20−22]

Although a crystal surface may reach the critical limit, leading to an apparent dissolution suppression, thermodynamics requires that it cannot stop in an absolute sense in an undersaturated solution but it may be too slow to be detected by CC. It is suggested that dissolution consists of at least two parts: one, the narrowly defined decrease in length of screw and dislocation lines, and the other, the surface rearrangement or the movement of the dislocations themselves, disappearing and renucleating during the reaction. Although dissolution almost stops, reaching an "equilibrium state", the movement of the dislocations on the

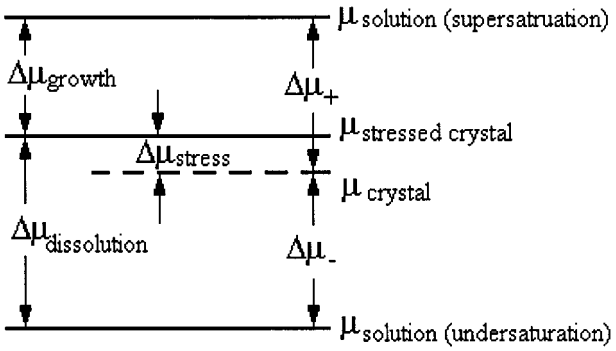

Figure 10. Chemical potentials of the ideal crystal, $\mu_{crystal}$, and solution, $\mu_{solution}$, at supersaturation and undersaturation; $\Delta\mu_+$ and $\Delta\mu_-$ are the changes of chemical potential for the ideal crystals during growth and dissolution, respectively. $\Delta\mu_{stress}$ is the increase of the chemical potential in the stressed (real) crystal. making the values of $\Delta\mu$ in real growth ($\Delta\mu_{growth}$) and dissolution ($\Delta\mu_{dissolution}$) processes lower and higher, respectively, than "ideal".

surfaces continues extremely slowly, driven by thermodynamic undersaturation requirements. Thus, since the critical condition for dissolution suppression cannot be sustained indefinitely, dissolution then resumes until a new critical condition is reached, resulting in a stepwise dissolution process.[21] Another important consequence of this model is that it explains why crystals resulting from a suppressed dissolution experiment at higher undersaturations can dissolve to a new limit in solutions of lower undersaturation. The value of l_c at higher undersaturation is less than that at lower σ, so that when crystals remaining in a suppressed dissolution experiment are exposed to a solution of much lower undersaturation, l becomes less than l_c at low undersaturation. These states are clearly thermodynamically unstable, especially for suppressed crystallites from experiments at the highest undersaturations, and the dissolution steps may be eliminated or reorganized through surface rearrangement. The result is that dissolution, initiated by the dislocations, can resume and the low l values may induce the formation of new dislocation sites, enabling further dissolution to take place.

Recently CC, AFM, and SECM methods have been used to investigate similar interesting kinetic dissolution phenomena involving soluble salts in solutions far from their critical conditions. However, as shown in eq 2, the critical condition is related to the edge-free energy, γ, which, for the sparingly soluble salts, is much greater than that for soluble electrolytes such as sodium chloride.[52,53,57,58] As a result, the values of l_c are much larger and can be investigated by current SECM, CC, and AFM experimental techniques. Moreover, the sparingly soluble crystal seeds are sufficiently small so as to reach critical conditions more rapidly. In contrast, the edge-free energy values for soluble salts are very small, leading to much smaller l_c requirements.

Analogously, in the corresponding crystallization processes, the spontaneous nucleation of soluble salts always occurs when the supersaturation slightly exceeds unity, but for some calcium phosphates, nucleation is not observed even at $\sigma > 5$. The changes of chemical potential, $\Delta\mu_+$ and $\Delta\mu_-$ for ideal perfect crystals during growth and dissolution, respectively, are illustrated in Figure 10. However, for real crystals, the chemical potential near dislocations is greater by the term $\Delta\mu_{stress}$.[11] Therefore, in the latter case, the absolute value of the supersaturation acting upon the central part of a spiral during growth is greater than the corresponding undersaturation value during dissolution. This implies that the absolute value of Δg for dissolution is greater than that for growth, making the critical dissolution conditions for soluble salts more difficult to attain. Moreover, the sizes of soluble crystals used for dissolution studies are always in the millimeter or larger range, whereas for sparingly soluble salts, with relatively small size and high l_c, the crystals attain critical conditions more readily, and the "abnormal" dissolution phenomena become more apparent. Thus, dissolution models developed for soluble systems may be inappropriate for application to sparingly soluble salts.

In terms of the model presented here, dissolution suppression is related to crystal size under specific dissolution conditions, with the same degree of undersaturaion, the size of the "suppressed" crystals being somewhat independent of the original crystal size. The SEM micrographs (in Supporting Information) show that the morphologies and sizes of the dissolution-suppressed crystallites are almost the same despite the difference in size of the original seed crystals. Thus, for the same crystal size, the dissolution percentage prior to suppression increases with σ. Furthermore, the critical conditions are related to the solubilities of the crystallites; the higher the solubility, the smaller the critical crystal size.

Conclusions

Dissolution deceleration and effective suppression and resumption have been investigated using a constant composition method. These phenomena cannot be explained in terms of current theories of crystal dissolution, in which critical conditions are not taken into account. It is suggested that one of the first steps of dissolution is the formation of pits/steps on crystal surfaces, increasing surface roughness and edge-free energy during the overall size reduction. When the size is reduced to that required by the critical conditions, effective rate suppression is observed in the constant composition experiments. These suggestions are supported by SEM and AFM data. Since current solution theories are based on experiments involving soluble salts, these phenomena were not observed since the critical conditions were outside the range of the experimental techniques employed. In the present study, the concepts of critical radius and the movement of pits/dissolution steps are introduced into a new theory. The results will be of particular interest in the dissolution of biological and geological minerals.

Acknowledgment. We thank the National Institute of Dental Research for a grant (DE03223) in support of this project.

Supporting Information Available: Atomic force micrographs (Figures S1a−c) showing the formation of the active pits/dislocation lines on DCPD crystal surfaces. Figures S2a−c are AFMs showing effective dissolution termination. Figure S3 showing the resumed dissolution of "dissolution terminated" OCP crystallites after long time periods ($\sigma = 0.171$). Figures S4a,b, SEMs of dissolution-suppressed crystallites of small and large OCP seeds, respectively, at $\sigma = 0.171$. This material is available free of charge via the Internet at http://pubs.acs.org.

JA010064P

(57) Walton, A. G. *The Formation and Properties of Precipitates*; Wiley: New York, 1967.
(58) Wu, W.; Nancollas, G. H. *J. Solution Chem.* **1998**, *27*, 521.